NUCL SCI TECH (2017) 28:67
DOI 10.1007/s41365-017-0221-z

Diffusion characteristics of HTO and $^{99}TcO_4^-$ in compacted Gaomiaozi (GMZ) bentonite

Tsuey-Lin Tsai[1] · Shih-Chin Tsai[2] · Yu-Hung Shih[1] · Liang-Cheng Chen[1] ·
Chuan-Pin Lee[3] · Te-Yen Su[1]

Received: 5 July 2016 / Revised: 24 August 2016 / Accepted: 24 September 2016 / Published online: 31 March 2017

Abstract The characteristics of diffusion are essential to the transport of radionuclides through buffer/backfill materials, such as bentonite, which are commonly found in waste repositories. This study used through-diffusion techniques to investigate the diffusion behavior of HTO and $^{99}TcO_4^-$ on GMZ bentonite of various densities. Diffusion rates were calculated by measuring the diffusion coefficients (D_e, D_a), plotting breakthrough curves and interpreting experiment data. The apparent and effective diffusion coefficients of HTO ranged from $(1.68 \pm 0.40) \times 10^{-11}$ to $(2.80 \pm 0.62) \times 10^{-11}$ m^2/s and from $(4.61 \pm 1.28) \times 10^{-12}$ to $(16.2 \pm 2.50) \times 10^{-12}$ m^2/s, respectively. The apparent and effective diffusion coefficients of $^{99}TcO_4^-$ ranged from $(5.26 \pm 0.16) \times 10^{-12}$ to $(7.78 \pm 0.43) \times 10^{-12}$ m^2/s and from $(1.49 \pm 0.002) \times 10^{-12}$ to $(4.16 \pm 0.07) \times 10^{-12}$ m^2/s, respectively. The distribution coefficients of HTO and $^{99}TcO_4^-$ ranged from $(0.70 \pm 0.12) \times 10^{-2}$ to $(1.36 \pm 0.53) \times 10^{-2}$ mL/g and from $(1.12 \pm 0.06) \times 10^{-2}$ to $(5.79 \pm 2.22) \times 10^{-2}$ mL/g, respectively. The D_e and K_d values were shown to decrease with an increase in the bulk dry density of compacted bentonite. Our results show that HTO and ^{99}Tc could be considered non-sorbent radionuclides. The data obtained in this study provide a valuable reference for the safety assessment of waste repositories.

Keywords Distribution coefficient · Apparent diffusion coefficient · Effective diffusion coefficient · Compacted bentonite · Through-diffusion

1 Introduction

In Taiwan, six nuclear power reactors, four BWRs and two PWRs, were installed between 1978 and 1985. Dealing with the highly radioactive waste from these nuclear power plants (NPPs) has become a critical situation in Taiwan. In the 1980s, Taipower Company (TPC), the owner of the NPPs, initiated a study on the long-term deep geological disposal of spent nuclear fuels (SNFs), intended to go into operation in 2055 [1].

Technetium-99 (^{99}Tc) is a major product formed at a relatively high yield from the fission of ^{235}U and ^{239}Pu in nuclear reactors (approximately 6.1%). As a pure β-emitter ($E_{max} = 292$ keV) with a long half-life of 2.13×10^5 year, ^{99}Tc is released into the environment primarily through the processing of nuclear fuel and nuclear weapons testing [2]. Its easy migrating from disposal facilities via high mobility in ground and surface water greatly increases the threat of radioactive exposure [3].

The geological disposal of SNFs in Taiwan is based on the installation of a multi-barrier repository system, comprising a natural barrier of host rock and its surroundings (aquifers, biosphere), as well as an engineered barrier system, which, referred to as a near-field environment, protects the waste package and limits the migration of radionuclides in case of their release. We examined the

✉ Shih-Chin Tsai
sctsai@mx.nthu.edu.tw

[1] Chemistry Division, Institute of Nuclear Energy Research, No. 1000, Wenhua Rd., Jiaan Village, Longtan District, Taoyuan, China

[2] Nuclear Science and Technology Development Center, National Tsing Hua University, Hsinchu, China

[3] Department of Earth Sciences, National Cheng Kung University, No. 1, University Road, Tainan, China

bentonite found in Gaomiaozi in Inner Mongolia, China (denoted as GMZ bentonite), as the buffer/backfill material for the geological disposal repository aimed at containing high-level radioactive waste (HLW). It provides good absorption properties, high cation exchangeability, excellent swelling capacity, microporous structure and low permeability [4, 5]. In this paper, the major content of GMZ bentonite is clay (<5 μm) and the minor one is mineral debris with a grain size of 0.10–0.05 mm. The cation exchange capacity (CEC) is 72.70–83.40 meq/100 g [6, 7]. The sorption characteristics of radionuclides on bentonite are viewed as essential to the assessment of disposal repositories. This has led to extensive research on the sorption and/or diffusion of ^{99}Tc (or analogous Re) on bentonite [8–13].

Diffusion in porous media can be studied using the following methods: through-diffusion (TD), in-diffusion (ID), back-to-back diffusion, reservoir depletion, etc. [14]. The TD and ID are typical standard laboratory techniques for testing the diffusion of radionuclides (RNs) using small, thin samples. TD tests allow direct measurement of the actual diffusion of RNs (i.e., effective diffusivity, D_e). Furthermore, these methods are generally applicable to weakly sorbing tracers [15]. This study adopted the TD method, using reservoirs with constant inlet concentration and constant outlet concentration. This approach is based on an approximate analytical solution assuming constant inlet and outlet concentrations, wherein the effective diffusion coefficient and rock capacity factor were estimated from steady-state measurements.

The diffusion coefficient is an important parameter in transport models used to evaluate the safety of waste repositories. In this paper, we begin by presenting the results of experiments dealing with the diffusion of HTO and ^{99}Tc through GMZ bentonite. We apply the accumulative concentration method developed by Crank [16] to obtain the distribution coefficient (K_d), apparent diffusion coefficient (D_a), effective diffusion coefficient (D_e) and retardation factor (R_f) in TD experiments using the two radionuclides addressed in this work.

2 Theory of through-diffusion

In this study, through-diffusion tests were used to determine the diffusion coefficient (D) in order to evaluate the transport of radionuclides through compacted media. If D is constant, then Fick's law applies:

$$\frac{\partial C}{\partial t} = D\left(\frac{\partial^2 C}{\partial x^2} + \frac{\partial^2 C}{\partial y^2} + \frac{\partial^2 C}{\partial z^2}\right). \tag{1}$$

If the compacted layer of bentonite is assumed to be homogeneous and isotropic, and the diffusion of the radionuclide occurs only in one dimension, then Eq. (1) can be rewritten as:

$$\frac{\partial C}{\partial t} = D_a \frac{\partial C^2}{\partial x^2}, \tag{2}$$

where $D_a = D_e/\alpha$ is the apparent diffusion coefficient; $\alpha = \theta + \rho_b K_d$ is the rock capacity factor, from which we can obtain the value of K_d according to bulk density (ρ_b) and porosity (θ); and C is the concentration in the liquid phase. The following initial and boundary conditions are given to describe the experimental constraints of the TD method:

$$C(x,0) = 0, \quad 0 < x < L,$$

$$C(0,t) = C_0,$$

$$C(L,t) = 0,$$

where C_0 is the concentration of tracer in the inlet reservoir and L is the sample thickness. For non-sorbing and sorbing tracers with a linear sorption isotherm, an analytical solution to the diffusion equation corresponding to the experimental arrangement is given in Ref. [16]. The total amount (Q_t) of diffusing radionuclides accumulated in the container (which was initially devoid of diffusing species) can be expressed as a function of time elapsed, t and x, as follows:

$$\frac{Q_t}{C_0} = \frac{\alpha A}{L}\left[D_a t - \frac{L^2}{6} - \sum_1^{\infty}(-1)^n \frac{2L^2}{n^2\pi^2}\exp\left(-\frac{D_a n^2 \pi^2 t}{L^2}\right)\right]. \tag{3}$$

As $t \rightarrow \infty$, the diffusion process reaches equilibrium, and the corresponding concentration ratio CR(t) can be rewritten as:

$$\mathrm{CR}(t) = \frac{\sum C_t}{C_0} = \frac{\alpha A}{VL}\left[D_a t_x - \frac{L^2}{6}\right], \tag{4}$$

where V and A are the volume and cross-sectional area of the compacted bentonite, respectively. CR(t) is a straight line with slope m and intersection t_x. Time-lag, t_x, is obtained from the intercept on the time axis of the breakthrough curve in Eq. (4). The graphical method developed by J. Crank is often used to determine D_a, D_e, R_f^{cal} (retardation factor) and K_d^{cal} (distribution coefficients) from the values of m, V, L, A, t_x, ρ_b and θ [17]:

$$D_a = L^2/(6t_x), \tag{5}$$

$$D_e = mVL/A, \tag{6}$$

$$R_f^{cal} = D_e/(\theta D_a) = 1 + \rho_b K_d^{cal}/\theta. \tag{7}$$

The total porosity of the sample, θ, is the ratio of the pore volume to the total volume of a representative sample of the medium. For a medium with a bulk dry density, ρ_b, and true density, ρ_t, the total porosity can be obtained using Eq. (8):

$$\theta = 1 - \rho_b/\rho_t. \tag{8}$$

3 Experimental

3.1 Geological material, tracer standards, chemicals and water phase

Na-bentonite was obtained from the Beijing Research Institute of Uranium Geology without further processing. The true density (ρ_t) of the GMZ bentonite was 2.7 g/cm^3. The aqueous phase used in the laboratory tests was synthetic groundwater (SGW). Table 1 lists the average values of anionic and cationic concentrations of underground water sampled from six boreholes at a site with crystalline host rock.

The ionic strength of groundwater in this area is approximately 2.35–2.93 mM. Tritiated water (HTO) was used as a conservative tracer, due to the fact that it is representative of all chemical elements that do not show retention in the solid phase. The standard solution used in this study could be traceable to Packard Spec-ChecTM and NIST SRM 4288A for HTO and $^{99}TcO_4^-$, respectively. The samples were measured using a liquid scintillation analyzer (LSA, Perkin Elmer Tri-Carb 3170 TR/SL) with counting efficiency of 91–92% of ^{99}Tc. Ten milliliters of the sample was combined with 10 mL scintillation cocktail (Ultima Gold^{TM} LLT and Ultima Gold^{TM} AB, Perkin Elmer, USA for HTO and ^{99}Tc, respectively) in a 20-mL polyethylene counting vial. All chemicals used in the experiments were of analytical purity, and deionized water (DIW) was used throughout the experiments.

3.2 Characterization

The specific surface area of the GMZ bentonite sample was determined using the N2-BET instrument (Micromeritics ASAP 2020). The chemical composition of GMZ bentonite was analyzed using a wavelength-dispersive X-ray fluorescence (WD-XRF) spectrometer (Axios, PANalytical Inc.). Analysis of the Na-bentonite crystals was performed using a Bruker D8 Advance diffractometer operated at 40 kV and 40 mA with a ceramic Cu X-ray (1.5418 Å) tube. Scanning was performed in the range of 5–80 2θ at a speed of 1°/min. A LynxEYE compound silicon strip detector with lower background (<0.1 cps) was employed. Patterns were identified via comparison with JCPD standards. The Na-bentonite sample was prepared in pressed potassium bromide (KBr) pellets and characterized using Fourier transform infrared (FTIR) spectrometer (Horiba FT-730 spectrometer, Kyoto, Japan) over a frequency range from 4000 to 400 cm^{-1} at a resolution of 4 cm^{-1}.

3.3 Through-diffusion experiment

Samples of bentonite clay of various dry densities (1.2, 1.4, 1.6, 1.8 and 2.0 g/cm^3) were statically compacted using a lifting jack (providing uniaxial compressive force) into thin slabs of 3 mm in thickness with a cross-sectional area of 19.6 cm^2. The slabs were placed between two chambers filled with SGW (100 mL), one of which contained the diffusing radionuclide. The sample disks were sandwiched between the source and collection (sampling) reservoirs made of chemically inert polypropylene (PP) with excellent mechanical properties. Overall, the diffusion cell comprised three parts: a source reservoir, a compacted bentonite sample holder and a collection (sampling) reservoir. Figure 1 is a schematic illustration of the column units used in the through-diffusion experiments. The sample was fixed using two Teflon O-ring washers (5 cm outer diameter and 3.6 cm inner diameter, 2.9 cm thickness) and two porous filters (Φ5 cm × 0.7 cm) with reinforced PP material at both ends of the inlet and outlet reservoirs. The sample holder was firmly fastened by screw threads to the chamber units using a torque wrench to reduce the deformation of the cells, minimize diffusion resistance and avoid the swelling pressure induced by bentonite clay after being saturated with water. A commercially available microporous PVC–SiO_2 membrane (separator) with 40–50 nm pore size (Europe Amer-Sil^{TM}) was used to prevent the generation of colloids (average size of 300 nm) from the bentonite. Molecules of HTO or H_2O with a size of 2.75 Å and $^{99}TcO_4^-$ with a size of 5.04 Å were able to penetrate the membrane easily.

Diffusion experiments were carried out as follows:

1. Before being poured into the source reservoir, the SGW underwent equilibration with the solid phase of compacted bentonite over a period of 12 days, wherein

Table 1 Chemical composition (in mg/L) of the synthetic groundwater used in this study (pH 8.06, E_h 405.9 mV)

Na	SO_4	TIC	Si	Ca	K	F	Cl	NO_3	PO_4	Zn	Mn	Fe	Mg	Al	NO_2
57.00	25.25	15.22	7.20	7.40	0.70	7.65	16.80	0.15	0.50	0.01	0.01	0.01	0.70	0.10	0.10

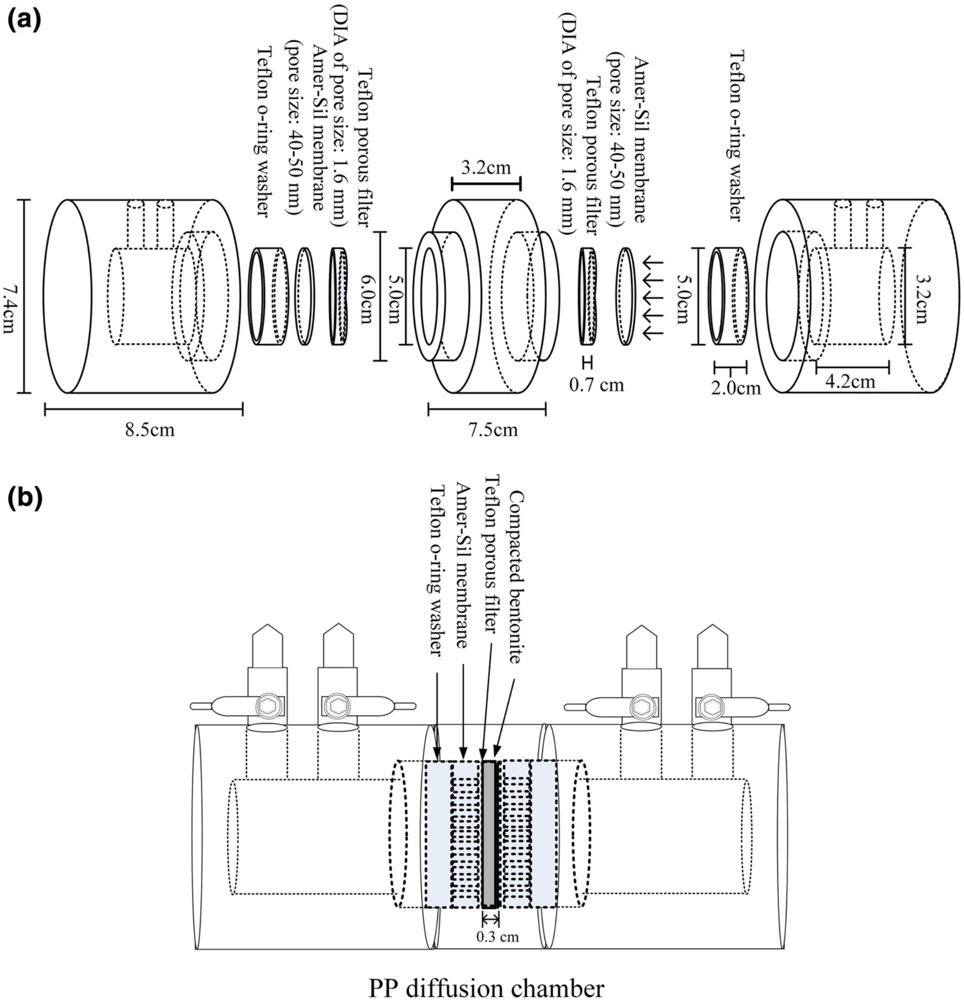

Fig. 1 Schematic drawing of diffusion chamber (in mm)

an air pump was used to create suction pressure of 2–3 kg/cm^2 to enable the injection of a large volume of water into the source reservoir in order to accelerate saturation;

2. Following water saturation, a very small volume of inactive tracer solution and HTO-spiked SGW were poured into the source reservoir and maintained at a fixed concentration of approximately 280 dpm/mL;
3. Samples of 10 ml were obtained from the collection reservoir (initially devoid of radioisotopes) at definite intervals, while the source tank underwent circulation for 30 min using a peristaltic pump;
4. The HTO concentration was tested using LSA; and
5. The HTO source reservoir was replaced by SGW spiked with ^{99}Tc radionuclide and maintained at a fixed concentration of approximately 1180 dpm/mL, whereupon Steps (3) and (4) were repeated.

The experimental setup included five through-diffusion chambers for dry densities of 1.2, 1.4, 1.6, 1.8 and 2.0 g/cm^3 (Fig. 2).

The experiments were carried out at room temperature. The volume of the inlet reservoir was sufficient to maintain the concentration at a near constant level (within a few percent) throughout the experiments. When the diffusion experiment was started, the solution in the collection reservoir was replaced with fresh solution (SGW) at regular time intervals (daily). The replaced solution was collected and measured using LSA to analyze the concentration of HTO and ^{99}Tc, which had diffused out from the bentonite. The quantities of individual radionuclides obtained in each collection and the accumulated concentration ratio *CR*(*t*) were plotted against the elapsed time t to yield through-diffusion curves.

4 Results and discussion

4.1 Characterization

The N2-BET surface area of the GMZ bentonite sample was 26 m^2/g. XRF analysis results show that the chemical

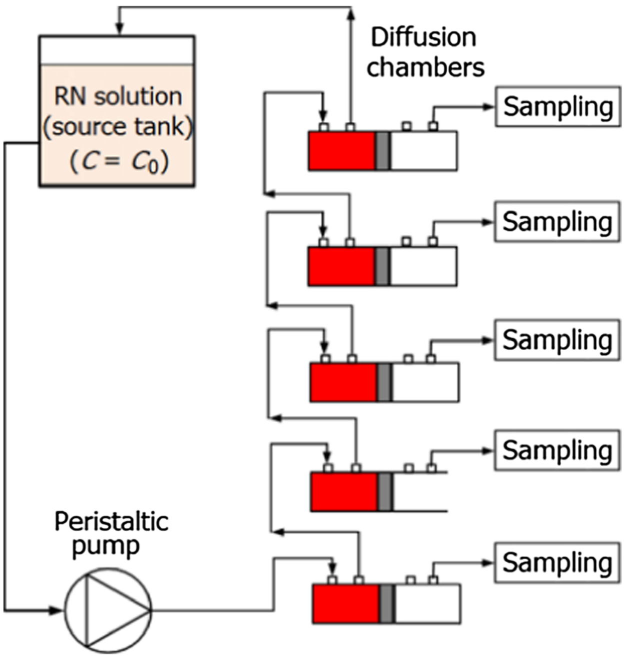

Fig. 2 Experimental setup for five through-diffusion chambers compacted to different dry densities (1.2, 1.4, 1.6, 1.8 and 2.0 g/cm^3)

composition was as follows: SiO_2, 63.71%; Al_2O_3, 13.44%; MgO, 2.67%; Fe_2O_3, 2.01%; Na_2O, 1.67%; CaO, 0.90%; K_2O, 0.67%; TiO_2, 0.12%; MnO, 0.04%; P_2O_5, 0.03%; and LOI, 12.91%.

Figure 3a shows XRD patterns of the Na-bentonite, indicating that it is composed primarily of montmorillonite (marked as M). The other peaks indicate impurities corresponding to quartz (Q), albite (A), a type of feldspar, and sodium aluminum silicate (S). Figure 3b shows the FTIR spectrum of Na-bentonite. The absorption band at 3634 cm^{-1} indicates the stretching vibrations of structural OH groups (Si–OH) in the GMZ bentonite. Free water molecules in bentonite produce a broad band at 3430 cm^{-1}, corresponding to H_2O-stretching vibrations. The band at 1643 cm^{-1} is associated with an overtone of the bending vibration of water. The band at 795 cm^{-1} confirms the presence of quartz, and the bands at 536 and 477 cm^{-1} are attributed to Al–O–Si and Si–O–Si bending vibrations, respectively. The very strong absorption band at 1047 cm^{-1} is associated with Si–O bending vibrations [18].

4.2 Diffusion of HTO and ^{99}Tc

The activity concentrations of tritium (HTO) and ^{99}Tc were measured and the accumulative concentration curves are plotted as a function of diffusion time. The diffusion curves yielded by $\sum C_t/C_0$ versus time agree with the theoretical breakthrough curves (BTCs), as shown in Fig. 4. The BTCs can be divided into two parts: (a) the transient period in which the concentrations build across the sample and (b) the period of steady-state diffusion in which the concentration in the measurement chamber increases steadily following the asymptote, i.e., a linear increase is observed over time.

It should be noted that Eq. (4) is valid only for the steady-state condition. As long as the diffusion process remains in the transient stage, the values of D_a and R_f, obtained from Eqs. (3) and (4), deviate. The dimensionless parameter, $t_d = D_a t_f / L^2$, is introduced here to determine whether the diffusion process reaches equilibrium. Crank [16] claimed that steady-state diffusion is achieved when t_d exceeds 0.45. As listed in Tables 2 and 3, all the t_d values for the HTO and ^{99}Tc in each column are greater than 0.45, indicating that the experiment time was of sufficient duration to reach steady-state diffusion. The diffusion parameters calculated from Eq. (4) are also listed in Tables 2 and 3, which summarize the through-diffusion experiments involving compacted bentonite (0.3 cm slabs) of various densities. The apparent and effective diffusion coefficients of HTO ranged from $(1.68 \pm 0.40) \times 10^{-11}$ to $(2.80 \pm 0.62) \times 10^{-11}$ m^2/s and from $(4.61 \pm 1.28) \times 10^{-12}$ to $(16.2 \pm 2.50) \times 10^{-12}$ m^2/s, respectively. The apparent and effective diffusion coefficients of $^{99}TcO_4^-$ ranged from $(5.26 \pm 0.16) \times 10^{-12}$ to $(7.78 \pm 0.43) \times 10^{-12}$ m^2/s and from $(1.49 \pm 0.002) \times 10^{-12}$ to $(4.16 \pm 0.07) \times 10^{-12}$ m^2/s, respectively. The distribution coefficients of HTO and $^{99}TcO_4^-$ ranged from $(0.70 \pm 0.12) \times 10^{-2}$ to $(1.36 \pm 0.53) \times 10^{-2}$ mL/g and from $(1.12 \pm 0.06) \times 10^{-2}$ to $(5.79 \pm 2.22) \times 10^{-2}$ mL/g, respectively. Our results from experiment dealing with diffusion parameters are comparable to those obtained in Refs. [10, 11, 19, 20]. The difference between our values and those in previous work can be attributed to differences in ionic strength and pH value of the liquid phase, the use of different types of bentonite, variations in the selection of steady-state regions on the diffusion breakthrough graphs, linear regression of the points along the line and errors due to counting statistics [21].

In this study, HTO was shown to access the total pore volume of the geological materials, which is equivalent to the water content; therefore, this was used as a conservative tracer. As shown in Table 2, the porosity values ($\theta_{exp} = D_e/D_a$) calculated from the diffusion measurements for HTO were similar to the theoretical value for total porosity (θ_{cal}). This implies that all the pores in the compacted bentonite were available for the mass transfer of neutral species [22]. ^{99}Tc is heptavalent and anionic in an oxidizing environment (as pertechnetate $^{99}TcO_4^-$). There was very little or no sorption of technetium on bentonite under these experimental conditions, due to exclusion effect of bentonite with a negative surface charge. As

Fig. 3 XRD patterns (**a**) and FTIR spectrum (**b**) of the GMZ bentonite

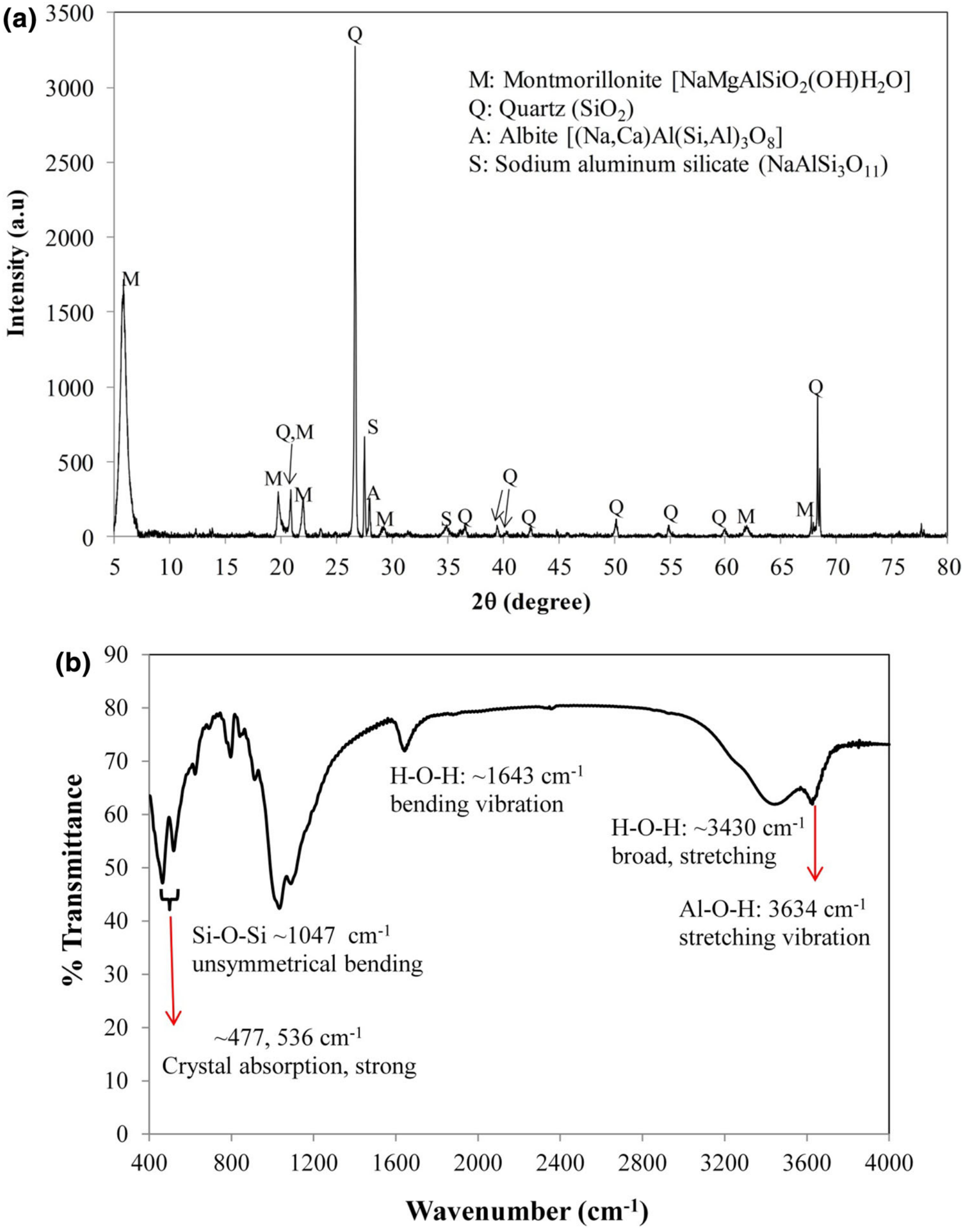

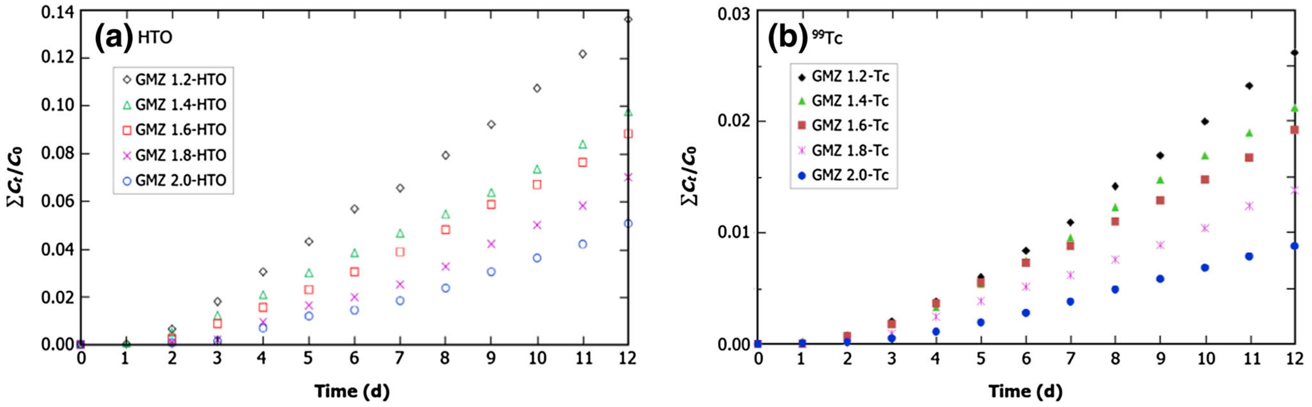

Fig. 4 Breakthrough curves of **a** HTO and **b** ^{99}Tc in the compacted bentonite with dry densities of 1.2, 1.4, 1.6, 1.8 and 2.0 g/cm^3

Table 2 Diffusion parameters of non-reactive tracer (HTO) in compacted GMZ bentonite in different dry densities in the SGW using TD tests

Items	GMZ 1.2	GMZ 1.4	GMZ 1.6	GMZ 1.8	GMZ 2.0
ρ_b (g/cm^3)	1.2	1.4	1.6	1.8	2.0
V (cm^3)	87	87	87	87	84
θ_{cal}	0.56	0.48	0.41	0.33	0.26
θ_{exp}	0.58	0.50	0.43	0.34	0.27
D_a (10^{-11} m^2/s)	2.80 ± 0.62	2.23 ± 0.30	1.95 ± 0.51	2.36 ± 0.53	1.68 ± 0.40
D_e (10^{-12} m^2/s)	16.2 ± 2.50	11.1 ± 1.11	8.31 ± 2.67	8.07 ± 0.95	4.61 ± 1.28
$^1R_f^{cal}$	1.03	1.03	1.04	1.04	1.05
$^2K_d^{cal}$ (10^{-2} mL/g)	1.36 ± 0.53	1.18 ± 0.68	0.97 ± 0.23	0.69 ± 0.09	0.70 ± 0.12
^3t_d	3.77	3.00	2.63	3.17	2.26

^{1} $R_f^{cal} = D_e/(\theta D_a)$; ^{2} $K_d = (R_f - 1)\theta/\rho_b$; ^{3} $t_d = Da\ t_f/L^2$; $L = 0.3$ cm; $A = 19.625$ cm^2

Table 3 Diffusion parameters of ^{99}Tc in compacted GMZ bentonite samples of different dry densities in the SGW using TD tests

Items	GMZ 1.2	GMZ 1.4	GMZ 1.6	GMZ 1.8	GMZ 2.0
ρ_b (g/cm^3)	1.2	1.4	1.6	1.8	2.0
V (cm^3)	87	87	87	87	84
θ_{cal}	0.56	0.48	0.41	0.33	0.26
D_a(10^{-12} m^2/s)	6.60 ± 0.66	6.66 ± 0.71	7.09 ± 0.37	7.78 ± 0.43	5.26 ± 0.16
D_e(10^{-12} m^2/s)	4.16 ± 0.07	3.39 ± 0.25	3.08 ± 0.28	2.76 ± 0.36	1.49 ± 0.002
$^1R_f^{cal}$	1.12	1.11	1.06	1.07	1.09
$^2K_d^{cal}$ (10^{-2} mL/g)	5.79 ± 2.22	3.71 ± 1.36	1.53 ± 0.78	01.37 ± 0.36	1.12 ± 0.06
^3t_d	0.76	0.77	0.82	0.90	0.61

^{1} $R_f^{cal} = D_e/(\theta D_a)$; ^{2} $K_d = (R_f - 1)\theta/\rho_b$; ^{3} $t_d = D_a\ t_f/L^2$

shown in Tables 2 and 3, the K_d value decreased with increasing dry density. The differences may be attributed to the fact that HTO and $^{99}TcO_4^-$ ions are unable to enter small occluded pores, thereby preventing them access to the entire volume, i.e., all the sorption sites in the compacted bentonite [13].

As the diffusion coefficient depends on the size and shape of molecules and interaction with solvent, the diffusion coefficients of $^{99}TcO_4^-$ are significantly smaller than those of HTO due to the larger radius of the hydrated anion (~0.35 nm for $^{99}TcO_4^-$) [22]. It can be also explained by changes in the species of ^{99}Tc during diffusion. The GMZ bentonite used in these experiments was untreated; therefore, it contained Fe-bearing minerals associated with minerals such as magnetite, hematite and goethite, which could significantly slow the mass transport of ^{99}Tc by reducing Tc(VII) to Tc(IV) as aqueous (Fe^{2+}) or solid [Fe(II)] [20]. Some $^{99}TcO_4^-$ could be transformed into insoluble $TcO_2 \cdot nH_2O$ [12, 23]. According to XRF data, 2.01% of the Fe_2O_3 in this study was contained in the GMZ bentonite; however, the mechanism underlying the reaction of iron oxide and Tc(VII) has yet to be fully elucidated. Figure 5 shows that a higher density leads to lower D_e values for HTO and ^{99}Tc. Both radionuclides appear to resist migration due to the constrictivity and tortuosity of the bentonite pores, which are directly related to the compaction pressure [21].

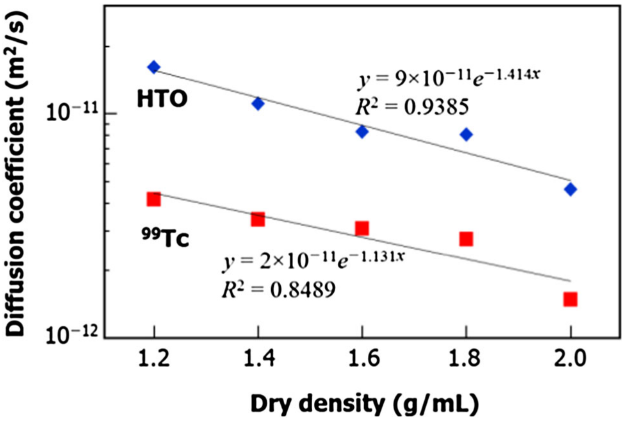

Fig. 5 Effective diffusion coefficient of HTO and technetium as a function of dry density

5 Conclusion

Our results show that the diffusion curves yielded by $\sum C_t/C_0$ against time are in agreement with the theoretical breakthrough curves. Under an oxidizing environment, technetium exists as negatively charged pertechnetate species ($^{99}TcO_4^-$), which is very poorly sorbed on bentonite ($K_d < 0.1$ mL/g) due to the anion exclusion effect associated with the negative surface charge of the bentonite particles. In through-diffusion tests, the effective diffusion coefficients of technetium ranged from 1.49×10^{-12} to 4.16×10^{-12} m^2/s when the dry densities of compacted bentonite were in the range of 1.2–2.0 g/cm^3. For HTO and ^{99}Tc, the decrease in K_d and D_e values with an increase in dry density was greatly affected by the pore structure of the compacted bentonite. Thus, GMZ bentonite is a promising candidate as a buffer/backfill material for nuclear waste aimed at the retardation of radionuclide diffusion.

Acknowledgements The authors would like to thank the Nuclear Backend Management Department at Taiwan Power Company for financially supporting this research.

References

1. Taiwan Power Company. Preliminary technical feasibility study for final disposal of spent nuclear fuel—2009 Progress Report (Summary), Taiwan, 2009. http://www.aec.gov.tw/webpage/control/waste/files/index_06_a8.pdf
2. T.K. Ikäheimonen, V.P. Vartti, E. Ilus et al., Technetium-99 in Fucusand seawater samples in the Finnish coastal area of the Baltic Sea, 1999. J. Radioanal. Nucl. Chem. **252**(2), 309–313 (2002). doi:10.1023/A:1015770423323
3. J.H. Chao, C.L. Tseng, C.L. Lee, Sequential extraction separation for determination of technetium-99 in radwastes by ICP-MS. J. Radioanal. Nucl. Chem. **251**(1), 105–112 (2002). doi:10.1023/A:1015054529857
4. Y.G. Chen, W.M. Ye, X.M. Yang et al., Effect of contact time, pH and ionic strength on Cd(II) adsorption from aqueous solution onto bentonite from Gaomiaozi, China. Environ. Earth Sci. **64**(2), 329–336 (2011). doi:10.1007/s12665-010-0850-6
5. Y.G. Chen, C.M. Zhu, Y.H. Sun et al., Adsorption of La(III) onto GMZ bentonite: effect of contact time, bentonite content, pH value and ionic strength. J. Radioanal. Nucl. Chem. **292**(3), 1339–1347 (2012). doi:10.1007/s10967-012-1612-6
6. X.D. Liu, T.A. Lug, G.P. Zhu, et al., Study on the properties of Gaomiaozi bentonite as the buffer/backfilling materials for HLW disposal (in Chinese). China Nuclear Information Centre, CNIC-01922 ECIT-000l, pp. 140–156. http://www.iaea.org/inis/collection/NCLCollectionStore/_Public/39/113/39113967.pdf
7. Y.M. Liu, G.Q. Xu, S.F. Liu, et al., Study on the basic property of Gaomiaozi bentonite, Inner Mongolia (in Chinese) China Nuclear Information Centre, CNIC-01552 BRIUG-0054, pp. 1–16. http://www.iaea.org/inis/collection/NCLCollectionStore/_Public/33/019/33019164.pdf
8. Y. Zhao, Z. Guo, J. Xu, $^{99}TcO_4^-$ diffusion and sorption in compacted GMZ bentonite studied by capillary method. J. Radioanal. Nucl. Chem. **298**, 147–152 (2013). doi:10.1007/s10967-012-2329-2
9. D.J. Liu, X.H. Fan, Adsorption behavior of ^{99}Tc on Fe, Fe_2O_3 and Fe_3O_4. J. Radioanal. Nucl. Chem. **264**(3), 691–698 (2005). doi:10.1007/s10967-005-0772-z
10. H. Wang, T. Wu, J. Chen et al., Effect of humic acid contact time on the diffusion of Re(VII) in GMZ bentonite. Nucl. Sci. Tech. **26**, S10314-1–S10314-5 (2015). doi:10.13538/j.1001-8042/nst.26.S10314
11. G.P. Xiao, T. Wu, H. Wang et al., Effect of inorganic salts on Se(IV) and Re(VII) diffusions in bentonite. Nucl. Sci. Tech. **26**, 050302-1–050302-5 (2015). doi:10.13538/j.1001-8042/nst.26.050302
12. H. Vinšová, P. Večerník, V. Jedináková-Křížová, Sorption characteristics of ^{99}Tc onto bentonite material with different additives under anaerobic conditions. Radiochim. Acta **94**, 435–440 (2006). doi:10.1524/ract.2006.94.8.435
13. X. Wang, Z. Tao, Diffusion of $^{99}TcO4^-$ in compacted bentonite: effect of pH, concentration, density and contact time. J. Radioanal. Nucl. Chem. **260**(2), 305–309 (2004). doi:10.1023/B:JRNC.0000027101.01834.1b
14. T.E. Eriksen, A. Jacobsson, Diffusion in clay. Experimental techniques and theoretical models. SKB TR 84-05, 1984, Svensk Kärnbränslehantering AB, Sweden. http://www.skb.com/publication/3179/TR84-05webb.pdf
15. C. Paul, Compilation of radionuclide sorption coefficients for performance assessment, SKB R-97-13, 1997, Svensk Kärnbränslehantering AB, Sweden. http://www.iaea.org/inis/collection/NCLCollectionStore/_Public/29/051/29051625.pdf
16. J. Crank, The mathematics of diffusion, 2nd edn. (Oxford, London (UK): Clarendon Press, 1975), pp. 50–52. http://www-eng.lbl.gov/~shuman/NEXT/MATERIALS&COMPONENTS/Xe_damage/Crank-The-Mathematics-of-Diffusion.pdf
17. C.P. Lee, S.C. Tsai, Y.L. Jan et al., Sorption and diffusion of HTO and cesium in crushed granite compacted to different lengths. J. Radioanal. Nucl. Chem. **275**(2), 371–378 (2008). doi:10.1007/s10967-007-6976-7
18. S.W. Wang, Y.H. Dong, M.L. He et al., Characterization of GMZ bentonite and its application in the adsorption of Pb(II) from aqueous solutions. Appl. Clay Sci. **43**, 164–171 (2009). doi:10.1016/j.clay.2008.07.028
19. Data report for the safety assessment SR-Site, SKB TR 10-52, p.p 163-169, December 2010, Svensk Kärnbränslehantering AB, Sweden. http://www.skb.com/publication/2166291/TR-10-52.pdf
20. J.Y. Li, W. Dai, G.P. Xiao et al., Pertechnetate diffusion in GMZ bentonite. J. Radioanal. Nucl. Chem. **293**, 763–767 (2012). doi:10.1007/s10967-012-1733-y
21. Z. Szántó, É. Svingor, M. Molnár et al., Diffusion of H-3, Tc-99, I-125, Cl-36 and Sr-85 in granite, concrete and bentonite. J. Radioanal. Nucl. Chem. **252**(1), 133–138 (2002). doi:10.1023/A:1015256308843
22. J.W. Yu, I. Neretnieks. Diffusion and sorption properties of radionuclides in compacted bentonite, SKB TR 97-12, 1997, Svensk Kärnbränslehantering AB, Sweden. http://www.iaea.org/inis/collection/NCLCollectionStore/_Public/29/015/29015600.pdf
23. Y.Y. Liu, C.X. Liu, R.K. Kukkadapu et al., ^{99}Tc(VII) retardation, reduction, and redox rate scaling in naturally reduced sediments. Environ. Sci. Technol. **49**, 13403–13412 (2015). doi:10.1021/acs.est.5b03273